

EchoVLA: Synergistic Declarative Memory for VLA-Driven Mobile Manipulation

Min Lin¹, Xiwen Liang¹, Bingqian Lin², Liu Jingzhi¹, Zijian Jiao¹, Kehan Li¹, Yu Sun¹, Weijia Liufu¹, Yuhan Ma¹, Yuecheng Liu³, Shen Zhao¹, Yuzheng Zhuang³, and Xiaodan Liang¹

¹ Shenzhen Campus of Sun Yat-sen University, Shenzhen, China

² Shanghai Jiao Tong University, Shanghai, China

³ Huawei Noah's Ark Lab, China
xdliang32@gmail.com

Abstract. Recent progress in Vision–Language–Action (VLA) models has enabled embodied agents to interpret multimodal instructions and perform complex tasks. However, existing VLAs are mostly confined to short-horizon, table-top manipulation, lacking the memory and reasoning capability required for mobile manipulation, where agents must coordinate navigation and manipulation under changing spatial contexts. In this work, we present EchoVLA, a memory-aware VLA model for mobile manipulation. EchoVLA incorporates a synergistic declarative memory inspired by the human brain, consisting of a scene memory that maintains a collection of spatial–semantic maps and an episodic memory that stores task-level experiences with multimodal contextual features. The two memories are individually stored, updated, and retrieved based on current observations, task history, and instructions, and their retrieved representations are fused via coarse- and fine-grained attention to guide base–arm diffusion policies. To support large-scale training, we further introduce MoMani, an automated benchmark that generates expert-level trajectories through multimodal large language model (MLLM)–guided planning and feedback-driven refinement, supplemented with real-robot demonstrations. Comprehensive simulated and real-world results demonstrate that EchoVLA substantially improves overall performance, e.g., it achieves the highest success rates of 0.52 on manipulation/navigation tasks and 0.31 on mobile manipulation tasks in simulation, exceeding the strong baseline $\pi_{0.5}$ by +0.20 and +0.11, respectively.

arXiv:2511.18112v2 [cs.RO] 6 Mar 2026

1 Introduction

Recent advances in Vision–Language–Action (VLA) models [2, 4, 12, 19, 21, 36, 40, 43, 52] have shown strong potential for general-purpose robot learning, enabling embodied agents to interpret multimodal inputs and perform diverse manipulation tasks. Models such as RT-2 [53], OpenVLA [23], and ManipLLM [27] demonstrate that large-scale vision–language pretraining can be extended to robot control, achieving impressive zero-shot generalization across unseen objects

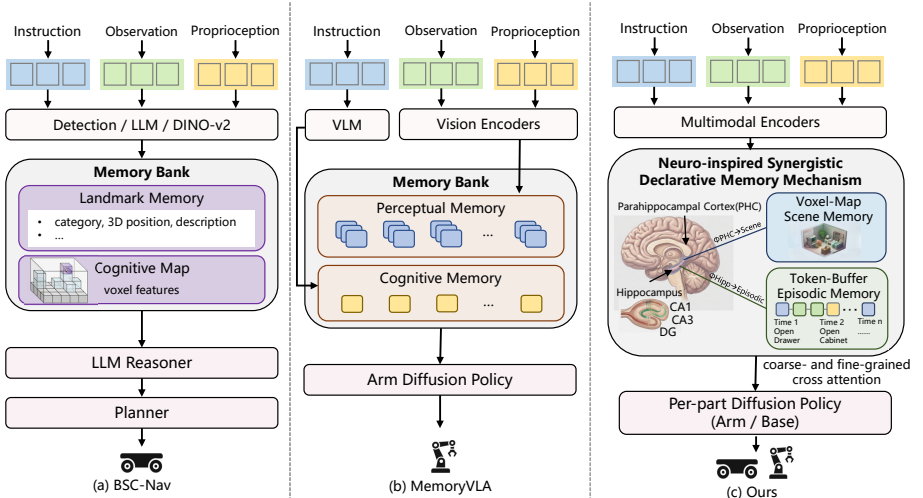


Fig. 1: Comparison of memory designs for mobile manipulation control. (a) BSC-Nav [38] uses a memory bank with landmark memory and a cognitive map to support LLM-based reasoning and planning. (b) MemoryVLA [39] builds a memory bank with perceptual memory and cognitive memory to condition a diffusion policy. (c) EchoVLA (ours) introduces dual memories: a persistent scene memory (voxel map) and a time-indexed episodic memory (token buffer), fused via coarse- and fine-grained cross attention for context-aware per-part diffusion control (arm/base).

and scenes. However, most existing VLAs are restricted to short-horizon, tabletop manipulation, and rely on Markovian control, where each decision depends solely on the current observation. This limitation prevents consistent reasoning over extended task sequences and hinders long-term spatial understanding.

To overcome this limitation, we draw inspiration from the declarative memory system in the human brain, which comprises complementary subsystems for spatial and experiential memory encoding, respectively. The parahippocampal cortex (PHC) and related retrosplenial regions represent the spatial and semantic structure of scenes, providing contextual information about environmental layouts and object relations [1, 14, 15]. These regions project to the hippocampus, which integrates contextual inputs into temporally organized episodic traces that capture individual experiences and task outcomes [13, 35]. Such a dual-system interaction allows humans to remember where things are and how tasks were accomplished—offering a useful analogy for memory-guided embodied reasoning.

Building on this insight, we propose **EchoVLA**, a memory-aware Vision–Language–Action model for mobile manipulation. EchoVLA introduces two complementary memories: a **scene memory** parallels the PHC by maintaining a persistent spatial representation as a voxel map, and an **episodic memory** mirrors hippocampal processing by storing time-indexed multimodal tokens to track task progress. As shown in Figure 1, prior work such as BSC-Nav [38] organizes memory as landmark descriptors and a cognitive map for LLM-based reasoning and planning, while MemoryVLA [39] builds perceptual and cognitive memories to condition diffusion control. In contrast, EchoVLA retrieves from

scene memory and episodic memory with separate coarse- and fine-grained cross attention, and fuses them to guide per-part diffusion policies (arm/base). This neuro-inspired dual-memory with attention-guided formulation helps maintain coherent spatial context and consistent task execution over long horizons.

We further introduce MoMani, an automated benchmark for mobile manipulation that generates expert-level trajectories via MLLM-guided planning and feedback-based refinement. Compared with existing mobile manipulation benchmarks—which remain limited in scale and task diversity—as well as datasets like RoboTwin 2.0 [8] and RoboCasa [31], MoMani offers richer task coverage and collects real-robot demonstrations on a holonomic mobile platform [47] to support large scale training.

Both simulation and real-world validation reveal that our EchoVLA maintains strong robustness in long-horizon mobile manipulation tasks by leveraging its synergistic declarative memory. On the RoboCasa [31] simulator, EchoVLA brings significant performance gain in SR over strong baseline $\pi_{0.5}$ [20] on manipulation/navigation tasks and mobile manipulation tasks by 0.20 and 0.11, respectively. Real-world experiments on the TidyBot++ platform [47] across a $7\text{m} \times 7\text{m}$ arena shows that EchoVLA achieves the highest SR of 0.44, outperforming $\pi_{0.5}$ [20] (0.33) and Diffusion Policy [9] (0.32).

Our contributions are summarized as follows:

- We propose EchoVLA, a neuro-inspired memory-aware VLA model equipped with synergistic scene and episodic memory for mobile manipulation.
- We introduce MoMani, an automated benchmark that provides expert-level multimodal trajectories with real-robot demonstrations for scalable embodied data generation.
- Extensive simulated and real-world results demonstrate that EchoVLA consistently outperforms strong baselines on various mobile manipulation tasks.

2 Related Work

2.1 Vision-Language-Action Model

Driven by advances in visual–language foundation models [6, 29, 34] and large-scale robot datasets [5, 32], Vision–Language–Action (VLA) models unify perception, reasoning, and control within a single multimodal policy. Representative works such as RT-2 [53], OpenVLA [23], and ManipLLM [27] discretize continuous actions into token sequences and perform autoregressive prediction, enabling large-scale pretraining but limiting motion continuity. Recent approaches (e.g., CogACT [26], DexVLA [45], HybridVLA [28]) introduce diffusion- or regression-based action heads to capture the multimodal distribution of robot trajectories, while AC-DiT [7] explicitly models coordination between the mobile base and the manipulator through adaptive diffusion. Notable works π_0 and $\pi_{0.5}$ [3, 20] address hierarchical trajectory diffusion for mobile manipulation. π_0 models the full robot action space, while $\pi_{0.5}$ introduces per-part decomposition for mobile

base and manipulator, adding partial episodic memory. Despite improved trajectory fidelity, both lack explicit scene-level memory for planning. Meanwhile, AnywhereVLA [17] adopts a modular design that combines classical SLAM with a fine-tuned VLA head for robust real-world pick-and-place, highlighting the practicality of hybrid systems. However, most existing VLAs remain Markovian, relying only on current observations without structured memory for reasoning.

In this work, we take inspiration from the memory system of human brain and propose EchoVLA, which constructs a synergistic declarative memory composed of scene and episodic memories. The scene memory explicitly builds a spatial-semantic map of object layouts and environmental structure, while the episodic memory records task-specific experience traces for contextual retrieval. This dual-memory mechanism enables reasoning in mobile-manipulation tasks beyond the capability of prior single-memory VLAs. A concurrent work MemoryVLA [39] augments VLAs with a perceptual-cognitive memory that caches visual features to enhance manipulation stability. However, its memory remains an implicit perceptual cache without an explicit spatial representation or task-level experience storage, limiting its ability for long-horizon task reasoning.

2.2 Mobile Manipulation Benchmark

Early embodied benchmarks such as RoboTHOR [10] for sim-to-real indoor navigation and iGibson 2.0 [24] for object-centric household tasks mainly offer mobile perception and basic interaction. Habitat 2.0 [42] further supports interactive rearrangement with articulated objects, but the mobile-manipulation coupling is still limited to predefined skills. Large-scale suites like BEHAVIOR-100 / 1K [25, 41] and ManiSkill2 [16] broaden the task families to 100–1000 household activities or 20+ manipulation families, yet most tasks assume a fixed or simplified manipulation setting rather than full mobile manipulation. More recent, robotics-oriented simulators move closer to real mobile manipulation: RoboCasa [31] targets realistic kitchen scenes with 120+ layouts and 2,500+ assets but the task spectrum is still mostly kitchen rearrangement; MoMa-Kitchen [51] provides 100K+ affordance-grounded samples for “last-mile” base positioning but is domain-specific to kitchens; RoboTwin 2.0 [8] automates data generation for 50 dual-arm tasks in 731-object settings but does not involve base navigation; TidyBot [46] shows LLM-guided, user-conditioned tidy-up on a mobile manipulator, while TidyBot++ [47] mainly contributes an open-source holonomic mobile-manipulation platform for data collection rather than a broad, automatic task generator. Different from existing benchmarks, our constructed MoMani provides a unified, automated pipeline that produces expert-level trajectories for diverse mobile-manipulation tasks and augments them with real-robot demonstrations.

3 EchoVLA

EchoVLA is a memory-augmented vision-language-action framework designed for mobile manipulation. Its key idea is to maintain two complementary memory

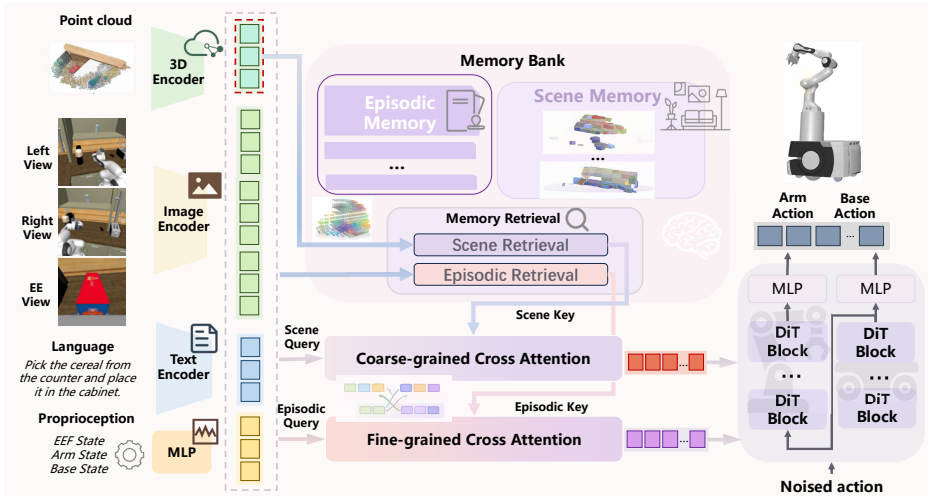


Fig. 2: Overview of EchoVLA. Multi-modal observations (RGB views, point clouds, language, and proprioception) are encoded into a unified token sequence. The model retrieves relevant information from both episodic and scene memory through coarse- and fine-grained cross-attention. The retrieved memory augments the diffusion policy, which generates base and arm actions through a per-part denoising process.

systems—scene memory and episodic memory—and integrate them into a coarse-to-fine retrieval hierarchy that improves spatial consistency, temporal reasoning, and manipulation precision. The overall architecture as illustrated in Figure 2 consists of: (1) multimodal state representation (Sec. 3.2), (2) memory retrieval and interaction (Sec. 3.3), and (3) diffusion-based action generation (Sec. 3.4). We first present the problem formulation of the mobile manipulation task in Sec. 3.1, then we describe each component of EchoVLA in detail.

3.1 Problem Formulation

At timestep t , the agent observes multi-view RGB-D images \mathcal{O}_t , proprioceptive states \mathbf{s}_t , and a natural-language instruction \mathcal{I} . The goal is to output continuous arm and base actions:

$$(a_t^{\text{arm}}, a_t^{\text{base}}) = \pi_\theta(\mathcal{I}, \mathcal{O}_{1:t}, \mathbf{s}_{1:t}). \quad (1)$$

We focus on non-Markovian tasks—two visually similar frames may correspond to completely different progress states (e.g., “cabinet opened” vs. “about to open”). Thus, a memory mechanism is needed.

3.2 Multimodal State Representation

EchoVLA encodes language, appearance, 3D structure, and robot configuration into a unified token sequence that drives memory retrieval and action generation. Each modality is processed with a dedicated backbone: language and multi-view RGB images use frozen SigLIP encoders [50], while 3D structure is modeled by a task-adaptive PointAttn network [44].

The instruction is encoded using the text tower of SigLIP, producing language tokens \mathbf{L} without updating the pretrained parameters. Multi-view RGB images from three fixed cameras are processed independently by the SigLIP vision tower, also kept frozen, yielding per-view features $\mathbf{V}_t^{(i)}$. These tokens preserve SigLIP’s cross-modal alignment, allowing the policy and memory modules to reason within a consistent semantic embedding space. The view-specific tokens are concatenated and projected into a shared feature space to form \mathbf{V}_t .

Depth observations are fused into a point cloud, which is encoded by a trainable PointAttn backbone. [44]. The resulting tokens \mathbf{P}_t provide fine-grained geometric cues—such as free-space structure, support surfaces, and object boundaries—and adapt to the specific robot embodiment and scene characteristics, complementing the frozen SigLIP features with manipulable 3D information.

The proprioceptive state \mathbf{s}_t is transformed into tokens \mathbf{R}_t using a small MLP, supplying the model with the robot’s internal configuration. We then form a unified token sequence:

$$\mathbf{S}_t = [\mathbf{L}, \mathbf{V}_t, \mathbf{P}_t, \mathbf{R}_t], \quad (2)$$

which serves as the query for hierarchical memory retrieval and conditions the diffusion policy.

3.3 Memory Retrieval and Interaction

EchoVLA maintains two complementary memory banks—scene memory and episodic memory—and retrieves information from them using a two-level hierarchical (coarse-to-fine) attention mechanism. The hierarchy comes from the semantic granularity of the two memories: scene memory provides slowly varying spatial structure, while episodic memory captures fine-grained, time-indexed task progress. The retrieved memory features are later fused with the current tokens and used to condition the diffusion policy.

Scene Memory Scene memory maintains a voxelized 3D feature map that accumulates spatial information across episodes within the same environment. Instead of storing features in temporal order, the memory represents a persistent, environment-specific 3D structure that is refined as new episodes unfold. At the beginning of training in a new environment, the memory is initialized as an empty voxel grid. As the agent interacts with the environment across multiple episodes, depth observations are aggregated into this voxel grid and encoded by the PointAttn network, producing a 3D feature volume (see Figure 3):

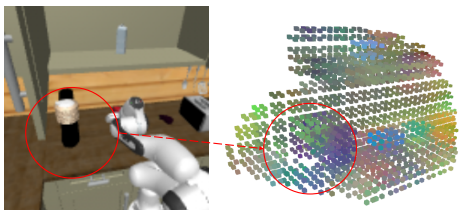


Fig. 3: Visualization of the voxelized 3D feature map, which encodes local geometric structure from depth observations.

As the agent interacts with the environment across multiple episodes, depth observations are aggregated into this voxel grid and encoded by the PointAttn network, producing a 3D feature volume (see Figure 3):

$$\mathbf{V}_t^{3D} \in \mathbb{R}^{X \times Y \times Z \times C}. \quad (3)$$

To incorporate new observations while avoiding redundant updates, the memory applies a discrepancy-driven rule: the current voxel features \mathbf{V}_t^{3D} are compared with a reconstruction generated from the existing memory. Regions whose reconstruction error exceeds a threshold are updated with the new PointAttn features, while unchanged areas retain their previous values. This update mechanism allows the scene map to evolve consistently across episodes, gradually converging to a stable representation of the environment’s geometry.

During inference, the scene memory continues to refine itself using the same discrepancy-based rule, enabling the model to adapt online if the environment differs from the training episodes or undergoes rearrangement. The resulting memory provides a compact but spatially coherent representation of the scene, capturing structural elements such as surfaces, free space, and container geometry that remain stable across episodes but are not fully observable in any single timestep.

Episodic Memory Episodic memory stores a short horizon of recent token sequences, each associated with its timestep. Formally, we maintain a time-indexed buffer:

$$\mathcal{M}^{\text{epi}} = \{(\mathbf{S}_{t-k}, t-k), \dots, (\mathbf{S}_{t-1}, t-1)\}, \quad (4)$$

where the window size k is determined by the memory capacity.

Unlike scene memory, which evolves slowly and captures stable 3D structure, episodic memory preserves fine-grained temporal information tied to recent interactions—such as whether a drawer has been opened, whether an object has already been grasped, or the precise end-effector configuration in the immediate past. The memory is maintained as a fixed-size FIFO buffer updated at each timestep, ensuring that temporally coherent information is retained while avoiding unbounded growth. By storing the original encoded tokens instead of compressing them into abstract summaries, the model preserves detailed temporal cues that are essential for resolving non-Markov ambiguities and maintaining consistent task execution across visually similar states.

Memory Matching and Attention EchoVLA accesses its two memory banks in two steps: it first matches the current representations to memory entries using cosine similarity, and then interacts with the selected entries via cross-attention.

For scene memory, the query is the current voxelized 3D feature map \mathbf{V}_t^{3D} . We compute cosine similarity between \mathbf{V}_t^{3D} and stored scene maps in $\mathcal{M}^{\text{scene}}$, select the top- k matches $\mathcal{M}_{\text{sel}}^{\text{scene}}$, and apply coarse cross-attention:

$$\mathbf{Z}_t^{\text{scene}} = \text{CrossAttn}(q = \mathbf{V}_t^{3D}, k / v = \mathcal{M}_{\text{sel}}^{\text{scene}}). \quad (5)$$

For episodic memory, the query is the current multi-modal state tokens \mathbf{S}_t . We match \mathbf{S}_t to historical states in \mathcal{M}^{epi} , select the most relevant subset $\mathcal{M}_{\text{sel}}^{\text{epi}}$, and apply fine cross-attention:

$$\mathbf{Z}_t^{\text{epi}} = \text{CrossAttn}(q = \mathbf{S}_t, k / v = \mathcal{M}_{\text{sel}}^{\text{epi}}). \quad (6)$$

The outputs of the two interactions are combined into a memory-augmented representation:

$$\mathbf{H}_t = [\mathbf{z}_t^{\text{scene}}, \mathbf{z}_t^{\text{epi}}], \quad (7)$$

which serves as the conditioning input for the diffusion-based action policy.

3.4 Diffusion-based Action Generation

To model the heterogeneous dynamics of mobile-base motion and arm manipulation, we propose a per-part diffusion policy conditioned on the memory-augmented representation \mathbf{H}_t .

Each action subspace $p \in \{\text{base}, \text{arm}\}$ is generated by an independent denoising diffusion process. For part p , the denoiser predicts the noise of a perturbed action sample:

$$\epsilon_\theta^{(p)} = \text{Denoiser}_p(\mathbf{z}_t, \mathbf{H}_t, t), \quad p \in \{\text{base}, \text{arm}\} \quad (8)$$

where \mathbf{z}_t is the noisy action at diffusion step t , \mathbf{H}_t captures the fused current observation with retrieved scene-level and episodic context.

During training, the objective minimizes the denoising loss for each part:

$$\mathcal{L} = \sum_{p \in \{\text{base}, \text{arm}\}} \mathbb{E}_{\mathbf{z}_t} [\|\epsilon - \epsilon_\theta^{(p)}(\mathbf{z}_t, \mathbf{H}_t, t)\|^2]. \quad (9)$$

This per-part design enables structured action generation, allowing coordinated yet decoupled learning of locomotion and manipulation behaviors, which improves scene generalization and cross-task transfer.

4 MoMani

We introduce **MoMani**, an automated benchmark for high-quality mobile manipulation data generation. As shown in Table 1, while frameworks like ManiSkill2 [16] and RoboCasa [31] focus on static tasks, MoMani provides a unified pipeline for integrated “navigation + manipulation” (Co-Gen) data.

Distinguishing itself from simulation-only platforms like BEHAVIOR-1K [25] and InfiniteWorld [37], MoMani uniquely incorporates both simulated (S) and real-robot (R) data sources. It stands as the only benchmark to support a full spectrum of automated generation modes across both Mobile-M (Sim) and Real-Robot platforms, delivering expert-level trajectories for complex, multi-stage embodied tasks.

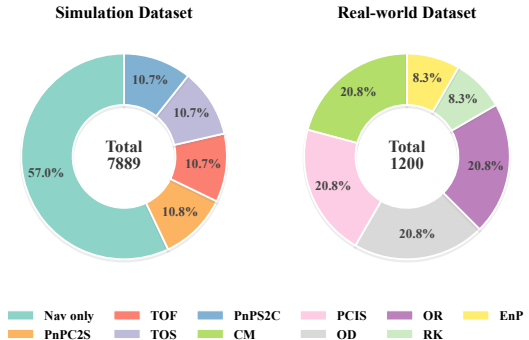


Fig. 4: Dataset composition across simulation and real-world tasks. The simulation set includes four mobile manipulation tasks (TOF, PnPS2C, PnPC2S, TOS) and a large pure-navigation subset. The real-world tasks (CM, OD, OR, PCIS, RK, EnP) involve mobile manipulation.

Table 1: Comparison of MoMani with other representative embodied AI platforms and datasets. The **Sub-tasks** column indicates the number of sub-tasks contained within each trajectory. In the **Data Source** column, *R* and *S* represent Real-world and Simulation data, respectively. In the **Generation** column, *Navigation*, *Manipulation*, and *Co-Gen* denote the automated programmatic generation of corresponding trajectories. In the **Robotic Platforms** column, **Mobile-M** refers to mobile manipulators in simulation environments, and **Real-Robot** indicates the availability of physical robot data or validation. In the **Action** column, *N* and *M* stand for Navigation and Manipulation.

Name	Sub-tasks	Data Source		Automated Generation			Robotic Platforms		Action
		Real (R)	Sim (S)	Navigation	Manipulation	Co-Gen	Mobile-M (Sim)	Real-Robot	
ManiSkill2 [16]	1-2	-	✓	-	✓	-	✓	-	<i>M</i>
Social Nav [33]	1	-	✓	-	✓	-	✓	-	<i>N, M</i>
HomeRobot [48]	3	-	✓	✓	✓	-	✓	✓	<i>N, M</i>
ProcTHOR [11]	3	-	✓	✓	✓	-	✓	-	<i>N, M</i>
Behavior-1K [25]	> 5	-	✓	✓	✓	-	✓	-	<i>N, M</i>
Open X-Embodiment [32]	1-3	✓	-	-	-	-	-	✓	<i>M</i>
RoboCasa365 [18]	2-16	-	✓	✓	✓	-	✓	-	<i>N, M</i>
InfiniteWorld [37]	3	-	✓	✓	✓	✓	✓	-	<i>N, M</i>
MoMani (Ours)	2-3	✓	✓	✓	✓	✓	✓	✓	<i>N, M</i>

4.1 Simulation Data Construction

As shown in Fig. 5, MoMani employs a two-stage automated pipeline to generate high-quality long-horizon trajectories.

Stage I: Online Candidate Generation. Task specifications are processed via an MMLM prompter to execute sequential Target-Aligned Sampling (L1), Safety-Aware Navigation (L2), and Continuous Nav-Manip Stitching (L3). Crucially, our engine supports simultaneous base and arm execution, utilizing continuous collision detection to generate coordinated “nav-manip” trajectories. Candidates must pass Hard Quality Gates—verifying zero collisions, precise alignment ($\Delta\text{pos} < 0.05\text{m}$, $\Delta\text{ori} < 5^\circ$), and 100% task success—before entering the feasible pool D_{pool} .

Stage II: Offline Selection & Audit. Candidates in D_{pool} undergo Lexicographic Ranking (L4) based on path length and planning cost to identify the expert-level Top-K set D_{topK} . A final Scene-Camera Audit ensures the dataset is training-ready, enabling the scalable generation of 5,000+ multimodal trajectories that bridge the gap between navigation and manipulation.

4.2 Real-Robot Demonstration Collection

To bridge the simulation-to-real gap, we collect a real-world dataset using a hardware configuration based on TidyBot++ [47]. Our platform features a Kinova Gen3 7-DoF manipulator on a holonomic mobile base, equipped with front RGB-D and top-view stereo cameras synchronized via ROS. We utilize a web-based teleoperation interface to record multimodal data streams at 30 Hz, which are then segmented into motion primitives. Successful trajectories are verified via replay, while failed attempts are discarded.

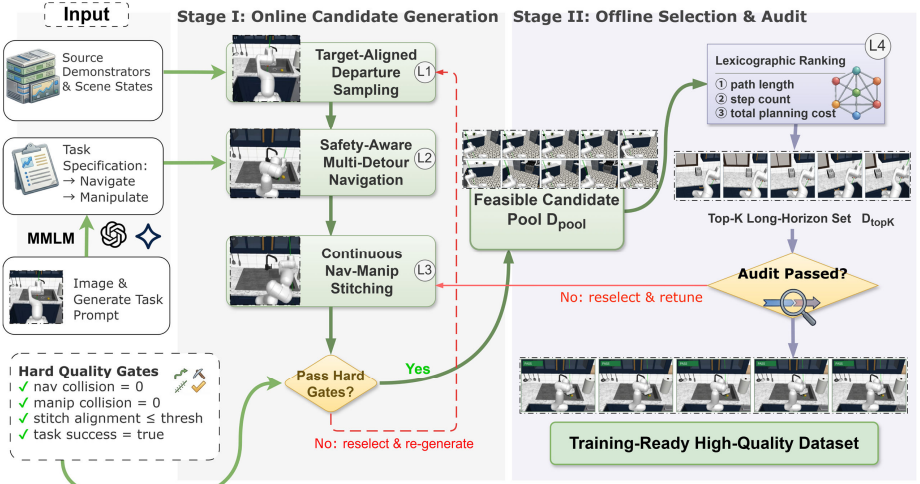


Fig. 5: Overview of the Quality-Controlled Data Engine. (I) *Online Candidate Generation* synthesizes trajectories filtered by hard quality gates (e.g., collision-free, task success). (II) *Offline Selection & Audit* ranks candidates via lexicographic criteria (path length, cost) to ensure a high-quality, training-ready dataset.

4.3 Dataset Distribution

As summarized in Figure 4, our dataset comprises:

- **Simulation (7,889 episodes):** Primarily consists of a large navigation-only subset (57.0%), supplemented by diverse mobile manipulation tasks including *PnPC2S* (PickPlaceCounterToStove, 10.8%), *PnPS2C* (PickPlaceSinkToCounter, 10.7%), *TOS* (TurnOnStove, 10.7%), and *TOF* (TurnOnSinkFaucet, 10.7%).
- **Real-world (1,200 episodes):** Features a balanced distribution (20.8% each) of manipulation tasks including *OR* (Open refrigerator door), *CM* (Close the microwave), *OD* (Open the drawer), and *PCIS* (Place the cup from the rack into the sink), along with additional tasks such as *EnP* (Enter the room and place the pears on the cabinet) and *RK* (Rotate the knob of a microwave) (8.3% each).

5 Experiment

5.1 Experimental Setup

We evaluate our proposed EchoVLA model in both simulation and real-world environments. In **simulation**, experiments are conducted in the RoboCasa simulator using multiple mobile manipulation tasks. For **real-world experiments**, we deploy EchoVLA using the *TidyBot++* platform [47] in a $7\text{m} \times 7\text{m}$ arena to execute diverse household tasks, notably *EnP* (Enter and Pick).

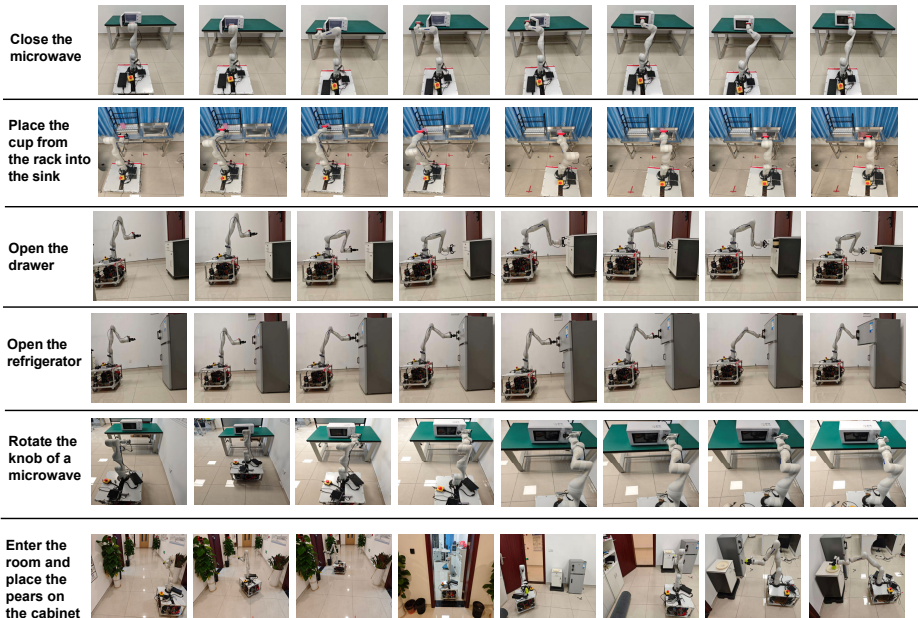


Fig. 6: Real-world rollouts generated by EchoVLA. The robot successfully completes four mobile manipulation tasks—turning off the microwave, placing the cup from the rack into the sink, opening the drawer, and opening the refrigerator.

Unlike other stationary or single-room tasks, *EnP* requires cross-room navigation and manipulation, moving from a starting corridor into a target room to retrieve objects. This validates the model’s capability in handling long-horizon spatial transitions and multi-stage logic in complex environments.

We train EchoVLA on 8 NVIDIA A100 GPUs with observations including multi-view RGB-D images and robot states. And the action space is decomposed into mobile base and arm actions following the per-part diffusion design.

5.2 Comparison with Baselines in RoboCasa Simulation

We evaluate **EchoVLA** against representative baselines including BC-T [30], Diffusion Policy [9], DP3 [49], $\pi_{0.5}$ [20], and WB-VIMA [22]. The evaluation spans four core tasks in the RoboCasa simulator: PickPlaceCounterToStove, PickPlaceSinkToCounter, TurnOnSinkFaucet, and TurnOnStove. To assess **Mobile Manipulation**, we introduce additional challenges by initializing the robot at a distance from targets or requiring follow-up navigation post-manipulation.

Performance is analyzed across three categories: (1) **Manipulation** (arm-only), (2) **Navigation** (base precision), and (3) **Mobile Manipulation** (coordinated control). We report the **Success Rate (SR)** averaged over three random seeds and 50 evaluation episodes per task. These findings are consolidated in Table 2, highlighting the inherent difficulty of coordinated mobile manipulation. The results in Table 2 reveal several important observations:

Table 2: Success Rate (SR) comparison on Manipulation, Navigation, and Mobile Manipulation tasks. EchoVLA (Ours) achieves the highest performance in most scenarios.

Category	Method	PnP C2S	PnP S2C	TOF	TOS	Nav only	Avg SR
Manip. / Nav.	BC-T	0.04	0.46	0.33	0.45	0.10	0.28
	Diffusion Policy	0.00	0.00	0.03	0.00	0.03	0.01
	DP3	0.03	0.25	0.43	0.26	0.13	0.22
	WB-VIMA	0.00	0.12	0.11	0.19	0.31	0.15
	$\pi_{0.5}$	0.18	0.20	0.44	0.52	0.24	0.32
	EchoVLA (Ours)	0.21	0.68	0.51	0.67	0.51	0.52
Mobile Manip.	BC-T	0.00	0.11	0.04	0.04	–	0.05
	DP3	0.00	0.10	0.08	0.04	–	0.06
	WB-VIMA	0.00	0.12	0.11	0.19	–	0.11
	$\pi_{0.5}$	0.08	0.25	0.18	0.27	–	0.20
	EchoVLA (Ours)	0.17	0.34	0.29	0.43	–	0.31

1) Method Comparison. For Manipulation and Navigation tasks, traditional behavior cloning (BC-T) and Diffusion Policy exhibit low performance, with Diffusion Policy often achieving near-zero success rates. $\pi_{0.5}$ shows improved performance, while our proposed EchoVLA achieves the highest average success rate (Avg Success = 0.52), demonstrating robust task execution.

2) Increased Difficulty in Mobile Manipulation. Coordinating base and arm control significantly increases complexity, causing success rates to drop across all methods. For instance, $\pi_{0.5}$ ’s average success decreases from 0.47 to 0.36, while BC-T exhibits a drastic decline from 0.28 to 0.05.

3) Superiority of EchoVLA. Despite the increased difficulty, EchoVLA maintains the highest success rate (0.31) in Mobile Manipulation tasks, outperforming all other methods. This highlights the method’s effectiveness in handling coordinated base–arm motion, long-range navigation, and sequential manipulation tasks.

4) Task-specific Performance Variations. Tasks such as PickPlaceSinkToCounter and TurnOnSinkFaucet show larger performance variations across methods, reflecting higher requirements for spatial understanding and precise manipulation. EchoVLA consistently achieves strong performance on these challenging tasks, demonstrating its capability in multi-modal perception and action reasoning.

5.3 Ablation Study

Ablations are performed on two representative RoboCasa tasks, **PnP Counter to Stove (Mobile)** and **PnP Counter to Stove**, and results are reported as **Success Rate (SR)** averaged over 50 episodes.

1) Observation Ablation. We examine the effect of removing point cloud input from the observation space. When the agent relies solely on RGB features without 3D geometric cues, its spatial grounding ability decreases notably. As shown in Table 3, removing point cloud input results in consistent performance

Table 3: Ablation results: Observation modalities and memory modules.

	RGB	PC	EM	SM	M	S
(a)	✗	✓	✓	✓	0.02	0.13
(b)	✓	✗	✓	✓	0.08	0.15
(c)	✓	✓	✓	✗	0.09	0.16
(d)	✓	✓	✗	✓	0.14	0.13
Ours	✓	✓	✓	✓	0.17	0.21

drops across both mobile and non-mobile variants, demonstrating the importance of geometric depth information for accurate object localization and grasping.

2) Memory Module Ablation. We further analyze the roles of our two memory mechanisms: **Episodic Memory (EM)** and **Scene Memory (SM)**. The ablation rows in Table 3 show that disabling either EM or SM leads to substantial degradation, and removing both RGB or PC signals further compounds these effects. Overall, the results highlight that observation diversity (RGB + PC) and hierarchical memory (EM + SM) are both essential for robust performance in manipulation and mobile manipulation tasks in RoboCasa.

3) Sensitivity Analysis. We evaluate EchoVLA’s sensitivity to EM window size L and update threshold τ . As shown in Table 4, a small L (2 or 4) leads to “plan forgetting” and oscillations, while $L = 16$ introduces latency with diminishing returns. $L = 8$ provides the optimal performance-efficiency balance. Furthermore, a low threshold ($\tau = 0.1$) causes representation instability, whereas a high threshold ($\tau = 0.7$) results in outdated scene memory. $\tau = 0.5$ strikes the best balance, ensuring memory freshness and stable spatial grounding for long-horizon tasks.

Table 4: Sensitivity analysis of hyperparameters on the PnPC2S (Mobile) task. $L = 8$ and $\tau = 0.5$ are selected as optimal values for EchoVLA.

Window Size(L)	2	4	8	16
SR \uparrow	0.08	0.12	0.17	0.15
Threshold (τ)	0.1	0.3	0.5	0.7
SR \uparrow	0.11	0.14	0.17	0.13

5.4 Real Robot Experiment

We evaluate EchoVLA across a diverse set of tasks, including opening a drawer (*OD*), closing a microwave (*CM*), placing a cup into the sink (*PCIS*), opening a refrigerator (*OR*), rotating a knob (*RK*), and entering a room to place pears (*EnP*). For each task, we conduct 20 independent trials with randomized initial robot base positions to ensure statistical significance.

1) Real-World Performance. As reported in Table 5, EchoVLA achieves a 0.44 mean success rate, outperforming $\pi_{0.5}$ (0.33) and Diffusion Policy (0.32). While baselines show efficacy in shorter or specific semantic tasks like *OD* and *OR*, EchoVLA demonstrates superior robustness in complex scenarios such as *CM* (0.70) and *RK* (0.50). Notably, it maintains a lead in the most challenging

long-horizon task, *EnP* (362.0 frames), confirming that our synergistic memory architecture effectively stabilizes control and mitigates perceptual noise in unconstrained environments.

Table 5: Success rates for real robot mobile manipulation tasks. We report performance on six basic actions. **Avg SR** is the mean success rate. (**Notes:** **OD**: Open the drawer, **CM**: Close the microwave, **PCIS**: Place the cup from the rack into the sink, **OR**: Open refrigerator door, **RK**: Rotate the knob of a microwave, **EnP**: Enter the room and place the pears on the cabinet.)

Method	OD	CM	PCIS	OR	RK	EnP	Avg SR
$\pi_{0.5}$	0.35	0.55	0.20	0.50	0.40	0.00	0.33
Diffusion Policy	0.40	0.60	0.50	0.30	0.10	0.03	0.32
EchoVLA (Ours)	0.45	0.70	0.50	0.40	0.50	0.10	0.44

2) Robustness to Real-World Perceptual Noise. As shown in Table 5, EchoVLA achieves a mean success rate of 0.44, surpassing Diffusion Policy (0.32). EchoVLA excels in long-horizon precision, achieving 50% SR on *RK* while baselines fail (10%) due to memory drift. This gap suggests that temporal context from EM acts as a corrective anchor, compensating for spatial inaccuracies like voxel map “ghosting” in SM.

3) Failure Analysis on Dynamic Occlusion. Despite its robustness, performance drops in *OR* due to dynamic occlusion. As the fridge door opens, rapidly changing geometry degrades EchoVLA’s explicit 3D Scene Memory. Conversely, baselines relying on implicit “muscle memory” are more robust to such blind spots where explicit geometry fails. This confirms that while synergistic memory ensures overall stability, explicit 3D representations remain sensitive to extreme structural dynamics.

6 Conclusion

We present EchoVLA, a memory-aware vision–language–action framework for mobile manipulation. EchoVLA combines a scene memory that preserves 3D spatial structure with an episodic memory that captures recent task context, enabling a memory-augmented diffusion policy to handle non-Markov decision-making and generalize across diverse tasks. We also introduce MoMani, a new benchmark covering both procedurally generated simulation tasks and real-robot evaluations. Extensive experiments demonstrate consistent improvements over strong baselines.

Limitations. EchoVLA’s performance is constrained by its reliance on high-quality depth and pose stream. In real-world deployments, cumulative odometry drift often leads to spatial misalignments or “ghosting” in the reconstructed Voxel Map within the Scene Memory. While our multi-memory architecture offers some robustness through cross-modal compensation, severe tracking errors during tasks remain a challenge. Future work will explore integrating loop-closure or visual-SLAM to further mitigate these perceptual inaccuracies.

References

1. Aminoff, E.M., Kveraga, K., Bar, M.: The role of the parahippocampal cortex in cognition. *Trends in cognitive sciences* **17**(8), 379–390 (2013)
2. Bjorck, J., Castañeda, F., Cherniadev, N., Da, X., Ding, R., Fan, L., Fang, Y., Fox, D., Hu, F., Huang, S., et al.: Gr00t n1: An open foundation model for generalist humanoid robots. arXiv preprint arXiv:2503.14734 (2025)
3. Black, K., Brown, N., Driess, D., Esmail, A., Equi, M., Finn, C., Fusai, N., Groom, L., Hausman, K., Ichter, B., Jakubczak, S., Jones, T., Ke, L., Levine, S., Li-Bell, A., Mothukuri, M., Nair, S., Pertsch, K., Shi, L.X., Tanner, J., Vuong, Q., Walling, A., Wang, H., Zhilinsky, U.: π_0 : A vision-language-action flow model for general robot control (2024), <https://arxiv.org/abs/2410.24164>
4. Brohan, A., Brown, N., Carbajal, J., Chebotar, Y., Dabis, J., Finn, C., Gopalakrishnan, K., Hausman, K., Herzog, A., Hsu, J., et al.: Rt-1: Robotics transformer for real-world control at scale. arXiv preprint arXiv:2212.06817 (2022)
5. Bu, Q., Cai, J., Chen, L., Cui, X., Ding, Y., Feng, S., Gao, S., He, X., Hu, X., Huang, X., et al.: Agibot world colosseum: A large-scale manipulation platform for scalable and intelligent embodied systems. arXiv preprint arXiv:2503.06669 (2025)
6. Caron, M., Touvron, H., Misra, I., Jégou, H., Mairal, J., Bojanowski, P., Joulin, A.: Emerging properties in self-supervised vision transformers. In: *Proceedings of the IEEE/CVF international conference on computer vision*. pp. 9650–9660 (2021)
7. Chen, S., Liu, J., Qian, S., Jiang, H., Li, L., Zhang, R., Liu, Z., Gu, C., Hou, C., Wang, P., et al.: Ac-dit: Adaptive coordination diffusion transformer for mobile manipulation. arXiv preprint arXiv:2507.01961 (2025)
8. Chen, T., Chen, Z., Chen, B., Cai, Z., Liu, Y., Li, Z., Liang, Q., Lin, X., Ge, Y., Gu, Z., et al.: Robotwin 2.0: A scalable data generator and benchmark with strong domain randomization for robust bimanual robotic manipulation. arXiv preprint arXiv:2506.18088 (2025)
9. Chi, C., Xu, Z., Feng, S., Cousineau, E., Du, Y., Burchfiel, B., Tedrake, R., Song, S.: Diffusion policy: Visuomotor policy learning via action diffusion (2024), <https://arxiv.org/abs/2303.04137>
10. Deitke, M., Han, W., Herrasti, A., Kembhavi, A., Kolve, E., Mottaghi, R., Salvador, J., Schwenk, D., VanderBilt, E., Wallingford, M., et al.: Robothor: An open simulation-to-real embodied ai platform. In: *Proceedings of the IEEE/CVF conference on computer vision and pattern recognition*. pp. 3164–3174 (2020)
11. Deitke, M., VanderBilt, E., Herrasti, A., Weihs, L., Ehsani, K., Salvador, J., Han, W., Kolve, E., Kembhavi, A., Mottaghi, R.: Proctor: Large-scale embodied ai using procedural generation. *Advances in Neural Information Processing Systems* **35**, 5982–5994 (2022)
12. Ding, P., Ma, J., Tong, X., Zou, B., Luo, X., Fan, Y., Wang, T., Lu, H., Mo, P., Liu, J., et al.: Humanoid-vla: Towards universal humanoid control with visual integration. arXiv preprint arXiv:2502.14795 (2025)
13. Eichenbaum, H.: On the integration of space, time, and memory. *Neuron* **95**(5), 1007–1018 (2017)
14. Epstein, R., Kanwisher, N.: A cortical representation of the local visual environment. *Nature* **392**(6676), 598–601 (1998)
15. Epstein, R.A.: Parahippocampal and retrosplenial contributions to human spatial navigation. *Trends in cognitive sciences* **12**(10), 388–396 (2008)
16. Gu, J., Xiang, F., Li, X., Ling, Z., Liu, X., Mu, T., Tang, Y., Tao, S., Wei, X., Yao, Y., et al.: Maniskill2: A unified benchmark for generalizable manipulation skills. arXiv preprint arXiv:2302.04659 (2023)

17. Gubernatorov, K., Voronov, A., Voronov, R., Pasynkov, S., Perminov, S., Guo, Z., Tsetserukou, D.: Anywherevla: Language-conditioned exploration and mobile manipulation (2025), <https://arxiv.org/abs/2509.21006>
18. He, Z., Zhang, Y., Zhou, Y., Tao, M., Li, H., Tian, Y., Zeng, J., Wang, T., Cai, W., Chen, Y., et al.: Nimbus: A unified embodied synthetic data generation framework. arXiv preprint arXiv:2601.21449 (2026)
19. Huang, W., Wang, C., Zhang, R., Li, Y., Wu, J., Fei-Fei, L.: Voxposer: Composable 3d value maps for robotic manipulation with language models. arXiv preprint arXiv:2307.05973 (2023)
20. Intelligence, P., Black, K., Brown, N., Darpinian, J., Dhabalia, K., Driess, D., Esmail, A., Equi, M., Finn, C., Fusai, N., Galliker, M.Y., Ghosh, D., Groom, L., Hausman, K., Ichter, B., Jakubczak, S., Jones, T., Ke, L., LeBlanc, D., Levine, S., Li-Bell, A., Mothukuri, M., Nair, S., Pertsch, K., Ren, A.Z., Shi, L.X., Smith, L., Springenberg, J.T., Stachowicz, K., Tanner, J., Vuong, Q., Walke, H., Walling, A., Wang, H., Yu, L., Zhilinsky, U.: $\pi_{0.5}$: a vision-language-action model with open-world generalization (2025), <https://arxiv.org/abs/2504.16054>
21. Jiang, Y., Gupta, A., Zhang, Z., Wang, G., Dou, Y., Chen, Y., Fei-Fei, L., Anandkumar, A., Zhu, Y., Fan, L.: Vima: General robot manipulation with multimodal prompts. arXiv preprint arXiv:2210.03094 **2**(3), 6 (2022)
22. Jiang, Y., Zhang, R., Wong, J., Wang, C., Ze, Y., Yin, H., Gokmen, C., Song, S., Wu, J., Fei-Fei, L.: Behavior robot suite: Streamlining real-world whole-body manipulation for everyday household activities (2025), <https://arxiv.org/abs/2503.05652>
23. Kim, M.J., Pertsch, K., Karamcheti, S., Xiao, T., Balakrishna, A., Nair, S., Rafailov, R., Foster, E., Lam, G., Sanketi, P., et al.: Openvla: An open-source vision-language-action model. arXiv preprint arXiv:2406.09246 (2024)
24. Li, C., Xia, F., Martín-Martín, R., Lingelbach, M., Srivastava, S., Shen, B., Vainio, K., Gokmen, C., Dharan, G., Jain, T., et al.: igibson 2.0: Object-centric simulation for robot learning of everyday household tasks. arXiv preprint arXiv:2108.03272 (2021)
25. Li, C., Zhang, R., Wong, J., Gokmen, C., Srivastava, S., Martín-Martín, R., Wang, C., Levine, G., Ai, W., Martinez, B., et al.: Behavior-1k: A human-centered, embodied ai benchmark with 1,000 everyday activities and realistic simulation. arXiv preprint arXiv:2403.09227 (2024)
26. Li, Q., Liang, Y., Wang, Z., Luo, L., Chen, X., Liao, M., Wei, F., Deng, Y., Xu, S., Zhang, Y., et al.: Cogact: A foundational vision-language-action model for synergizing cognition and action in robotic manipulation. arXiv preprint arXiv:2411.19650 (2024)
27. Li, X., Zhang, M., Geng, Y., Geng, H., Long, Y., Shen, Y., Zhang, R., Liu, J., Dong, H.: Manipllm: Embodied multimodal large language model for object-centric robotic manipulation. In: Proceedings of the IEEE/CVF Conference on Computer Vision and Pattern Recognition. pp. 18061–18070 (2024)
28. Liu, J., Chen, H., An, P., Liu, Z., Zhang, R., Gu, C., Li, X., Guo, Z., Chen, S., Liu, M., et al.: Hybridvla: Collaborative diffusion and autoregression in a unified vision-language-action model. arXiv preprint arXiv:2503.10631 (2025)
29. Liu, S., Zeng, Z., Ren, T., Li, F., Zhang, H., Yang, J., Jiang, Q., Li, C., Yang, J., Su, H., et al.: Grounding dino: Marrying dino with grounded pre-training for open-set object detection. In: European conference on computer vision. pp. 38–55 (2024)

30. Mandlekar, A., Xu, D., Wong, J., Nasiriany, S., Wang, C., Kulkarni, R., Fei-Fei, L., Savarese, S., Zhu, Y., Martín-Martín, R.: What matters in learning from offline human demonstrations for robot manipulation (2021), <https://arxiv.org/abs/2108.03298>
31. Nasiriany, S., Maddukuri, A., Zhang, L., Parikh, A., Lo, A., Joshi, A., Mandlekar, A., Zhu, Y.: Robocasa: Large-scale simulation of everyday tasks for generalist robots. arXiv preprint arXiv:2406.02523 (2024)
32. O'Neill, A., Rehman, A., Maddukuri, A., Gupta, A., Padalkar, A., Lee, A., Pooley, A., Gupta, A., Mandlekar, A., Jain, A., et al.: Open x-embodiment: Robotic learning datasets and rt-x models: Open x-embodiment collaboration 0. In: 2024 IEEE International Conference on Robotics and Automation (ICRA). pp. 6892–6903 (2024)
33. Puig, X., Undersander, E., Szot, A., Cote, M.D., Yang, T.Y., Partsey, R., Desai, R., Clegg, A.W., Hlavac, M., Min, S.Y., et al.: Habitat 3.0: A co-habitat for humans, avatars and robots. arXiv preprint arXiv:2310.13724 (2023)
34. Radford, A., Kim, J.W., Hallacy, C., Ramesh, A., Goh, G., Agarwal, S., Sastry, G., Askell, A., Mishkin, P., Clark, J., et al.: Learning transferable visual models from natural language supervision. In: International conference on machine learning. pp. 8748–8763 (2021)
35. Ranganath, C., Ritchey, M.: Two cortical systems for memory-guided behaviour. *Nature reviews neuroscience* **13**(10), 713–726 (2012)
36. Reed, S., Zolna, K., Parisotto, E., Colmenarejo, S.G., Novikov, A., Barth-Maron, G., Gimenez, M., Sulsky, Y., Kay, J., Springenberg, J.T., et al.: A generalist agent. arXiv preprint arXiv:2205.06175 (2022)
37. Ren, P., Li, M., Luo, Z., Song, X., Chen, Z., Liufu, W., Yang, Y., Zheng, H., Xu, R., Huang, Z., et al.: Infiniteworld: A unified scalable simulation framework for general visual-language robot interaction. arXiv preprint arXiv:2412.05789 (2024)
38. Ruan, S., Wang, L., Kang, C., Zhu, Q., Liu, S., Wei, X., Su, H.: From reactive to cognitive: brain-inspired spatial intelligence for embodied agents. *intelligence (AGI)* **3**(9), 10 (2025)
39. Shi, H., Xie, B., Liu, Y., Sun, L., Liu, F., Wang, T., Zhou, E., Fan, H., Zhang, X., Huang, G.: Memoryvla: Perceptual-cognitive memory in vision-language-action models for robotic manipulation. arXiv preprint arXiv:2508.19236 (2025)
40. Shridhar, M., Manuelli, L., Fox, D.: Cliport: What and where pathways for robotic manipulation. In: Conference on robot learning. pp. 894–906 (2022)
41. Srivastava, S., Li, C., Lingelbach, M., Martín-Martín, R., Xia, F., Vainio, K.E., Lian, Z., Gokmen, C., Buch, S., Liu, K., et al.: Behavior: Benchmark for everyday household activities in virtual, interactive, and ecological environments. In: Conference on robot learning. pp. 477–490 (2022)
42. Szot, A., Clegg, A., Undersander, E., Wijmans, E., Zhao, Y., Turner, J., Maestre, N., Mukadam, M., Chaplot, D.S., Maksymets, O., et al.: Habitat 2.0: Training home assistants to rearrange their habitat. *Advances in neural information processing systems* **34**, 251–266 (2021)
43. Team, O.M., Ghosh, D., Walke, H., Pertsch, K., Black, K., Mees, O., Dasari, S., Hejna, J., Kreiman, T., Xu, C., et al.: Octo: An open-source generalist robot policy. arXiv preprint arXiv:2405.12213 (2024)
44. Wang, J., Guo, D., et al.: Pointattn: You only need attention for point cloud completion. In: Proceedings of the AAAI Conference on Artificial Intelligence (2023)
45. Wen, J., Zhu, Y., Li, J., Tang, Z., Shen, C., Feng, F.: Dexvla: Vision-language model with plug-in diffusion expert for general robot control. arXiv preprint arXiv:2502.05855 (2025)

46. Wu, J., Antonova, R., Kan, A., Lepert, M., Zeng, A., Song, S., Bohg, J., Rusinkiewicz, S., Funkhouser, T.: Tidybot: Personalized robot assistance with large language models. *Autonomous Robots* **47**(8), 1087–1102 (2023)
47. Wu, J., Chong, W., Holmberg, R., Prasad, A., Gao, Y., Khatib, O., Song, S., Rusinkiewicz, S., Bohg, J.: Tidybot++: An open-source holonomic mobile manipulator for robot learning. arXiv preprint arXiv:2412.10447 (2024)
48. Yenamandra, S., Ramachandran, A., Yadav, K., Wang, A., Khanna, M., Gervet, T., Yang, T.Y., Jain, V., Clegg, A.W., Turner, J., et al.: Homerobot: Open-vocabulary mobile manipulation. arXiv preprint arXiv:2306.11565 (2023)
49. Ze, Y., Zhang, G., Zhang, K., Hu, C., Wang, M., Xu, H.: 3d diffusion policy: Generalizable visuomotor policy learning via simple 3d representations (2024), <https://arxiv.org/abs/2403.03954>
50. Zhai, X., Mustafa, B., Kolesnikov, A., Beyer, L.: Sigmoid loss for language image pre-training (2023), <https://arxiv.org/abs/2303.15343>
51. Zhang, P., Gao, X., Wu, Y., Liu, K., Wang, D., Wang, Z., Zhao, B., Ding, Y., Li, X.: Moma-kitchen: A 100k+ benchmark for affordance-grounded last-mile navigation in mobile manipulation. arXiv preprint arXiv:2503.11081 (2025)
52. Zhao, T.Z., Kumar, V., Levine, S., Finn, C.: Learning fine-grained bimanual manipulation with low-cost hardware. arXiv preprint arXiv:2304.13705 (2023)
53. Zitkovich, B., Yu, T., Xu, S., Xu, P., Xiao, T., Xia, F., Wu, J., Wohlhart, P., Welker, S., Wahid, A., et al.: Rt-2: Vision-language-action models transfer web knowledge to robotic control. In: *Conference on Robot Learning*. pp. 2165–2183 (2023)